



HAL
open science

Electrooptic and converse-piezoelectric properties of epitaxial GaN/Si structures for optoelectronic applications

Mireille Cuniot-Ponsard, Irma Saraswati, S.-M. Ko, Mathieu Halbwx, Y.-H. Cho, N.-R. Poespawati, El Hadj Dogheche

► **To cite this version:**

Mireille Cuniot-Ponsard, Irma Saraswati, S.-M. Ko, Mathieu Halbwx, Y.-H. Cho, et al.. Electrooptic and converse-piezoelectric properties of epitaxial GaN/Si structures for optoelectronic applications. European Materials Research Society Spring Meeting, E-MRS Spring 2014, Symposium K - Challenges for group III nitride semiconductors for solid state lighting and beyond, May 2014, Lille, France. hal-00961405

HAL Id: hal-00961405

<https://hal.science/hal-00961405>

Submitted on 16 Nov 2015

HAL is a multi-disciplinary open access archive for the deposit and dissemination of scientific research documents, whether they are published or not. The documents may come from teaching and research institutions in France or abroad, or from public or private research centers.

L'archive ouverte pluridisciplinaire **HAL**, est destinée au dépôt et à la diffusion de documents scientifiques de niveau recherche, publiés ou non, émanant des établissements d'enseignement et de recherche français ou étrangers, des laboratoires publics ou privés.



Electro-optic and converse-piezoelectric properties of epitaxial GaN grown on silicon by metal-organic chemical vapor deposition

M. Cuniot-Ponsard, I. Saraswati, S.-M. Ko, M. Halbwax, Y. H. Cho, and E. Dogheche

Citation: [Applied Physics Letters](#) **104**, 101908 (2014); doi: 10.1063/1.4868427

View online: <http://dx.doi.org/10.1063/1.4868427>

View Table of Contents: <http://scitation.aip.org/content/aip/journal/apl/104/10?ver=pdfcov>

Published by the [AIP Publishing](#)

Articles you may be interested in

[Effects of Al x Ga 1 - x N interlayer for GaN epilayer grown on Si substrate by metal-organic chemical-vapor deposition](#)

J. Vac. Sci. Technol. B **28**, 473 (2010); 10.1116/1.3385672

[GaN hybrid microcavities in the strong coupling regime grown by metal-organic chemical vapor deposition on sapphire substrates](#)

J. Appl. Phys. **101**, 093110 (2007); 10.1063/1.2728744

[Growth stresses and cracking in GaN films on \(111\) Si grown by metal-organic chemical-vapor deposition. I. AlN buffer layers](#)

J. Appl. Phys. **98**, 023514 (2005); 10.1063/1.1978991

[GaN homoepitaxial layers grown by metalorganic chemical vapor deposition](#)

Appl. Phys. Lett. **75**, 1276 (1999); 10.1063/1.124666

[Structural, optical, and surface acoustic wave properties of epitaxial ZnO films grown on \(0112\) sapphire by metalorganic chemical vapor deposition](#)

J. Appl. Phys. **85**, 2595 (1999); 10.1063/1.369577

The logo for AIP APL Photonics is displayed in a white font on a red background. The letters 'AIP' are large and bold, followed by a vertical bar and the words 'APL Photonics' in a smaller font.

AIP | APL Photonics

APL Photonics is pleased to announce
Benjamin Eggleton as its Editor-in-Chief



Electro-optic and converse-piezoelectric properties of epitaxial GaN grown on silicon by metal-organic chemical vapor deposition

M. Cuniot-Ponsard,^{1,a)} I. Saraswati,^{2,3} S.-M. Ko,⁴ M. Halbax,² Y. H. Cho,⁴ and E. Dogheche²

¹Laboratoire Charles Fabry, IOGS, CNRS, Univ Paris-Sud, 2 Avenue Augustin Fresnel, 91127 Palaiseau Cedex, France

²Department Optoelectronics, Institut d'Electronique, Microélectronique et Nanotechnologie, IEMN UMR 8520 CNRS, Avenue Poincaré, 59652 Villeneuve d'Ascq, France

³Electrical Engineering Department, Faculty of Engineering, University Indonesia, 42435 Depok, Indonesia

⁴Department of Physics and KI for the NanoCentury, Korea Advanced Institute of Science and Technology (KAIST), Daejeon 305-701, South Korea

(Received 19 February 2014; accepted 26 February 2014; published online 13 March 2014)

We report the measurement of the (r_{13} , r_{33}) Pockels electro-optic coefficients in a GaN thin film grown on a Si(111) substrate. The converse piezoelectric (d_{33}) and electro-absorptive coefficients are simultaneously determined. Single crystalline GaN epitaxial layers were grown with a AlGaIn buffer layer by metal organic chemical vapor deposition, and their structural and optical properties were systematically investigated. The electro-optic, converse piezoelectric, and electro-absorptive coefficients of the GaN layer are determined using an original method. A semi-transparent gold electrode is deposited on the top of the GaN layer, and an alternating voltage is applied between top and bottom electrodes. The coefficients are simultaneously and analytically determined from the measurement of the electric-field-induced variation $\Delta R(\theta)$ in the reflectivity of the Au/GaN/buffer/Si stack, versus incident angle and light polarization. The method also enables to determine the GaN layer polarity. The results obtained for a Ga-face [0001] GaN layer when using a modulation frequency of 230 Hz are for the electro-optic coefficients $r_{13} = +1.00 \pm 0.02$ pm/V, $r_{33} = +1.60 \pm 0.05$ pm/V at 633 nm, and for the converse piezoelectric coefficient $d_{33} = +4.59 \pm 0.03$ pm/V. The value measured for the electro-absorptive variation at 633 nm is $\Delta k_o/\Delta E = +0.77 \pm 0.05$ pm/V. © 2014 AIP Publishing LLC. [<http://dx.doi.org/10.1063/1.4868427>]

Due to their unique physical properties such as high band-gap (3.4 eV), high chemical, mechanical and thermal stability, high electron mobility and breakdown field, gallium nitride thin films are of particular interest for optoelectronic and high power – high frequency electronic applications (from blue light emitting diodes to high power switching devices).^{1,2} Epitaxial GaN is usually grown on sapphire or buffered silicon substrates.³ The latter are less expensive, can be made conductive, and offer the advantages of a mature Si-based technology. The integration of well-established Si electronics with GaN-based photonic devices is therefore a particularly attractive way to develop the next-generation of optoelectronic devices. Due to its wurtzite crystalline structure lacking inversion symmetry along the c -axis direction, GaN is also a highly polar, piezoelectric, and nonlinear optical semiconductor.⁴ These properties are of special interest for the current optoelectronic applications, but they also open the path to applications such as electro-optic modulation and wavelength conversion. A few measurements of the second order susceptibility $\chi_{ij}^{(2)}$ ⁵⁻¹⁰ and only two measurements of the electro-optic Pockels coefficients^{11,12} have been published for GaN grown on sapphire⁵⁻¹¹ or GaAs¹² substrates. This letter reports the first measurement of the Pockels electro-optic coefficients r_{13} and r_{33} for a GaN thin film grown on silicon. These electro-optic coefficients, together with the converse piezoelectric

(d_{33}) and electro-absorptive coefficients are determined analytically and simultaneously from the measurement of the electric-field-induced variation in the reflectivity of the GaN film sandwiched between the buffered Si substrate and a top gold electrode. Structural and optical properties of the film are presented prior to the electric-field induced properties.

Undoped GaN (u-GaN) was grown on an n-type silicon (111) substrate in a conventional showerhead type metal organic chemical vapor deposition (MOCVD) reactor (Sysnex Marvel 260 NT). To remove the natural oxide layer, the Si (111) substrates were cleaned in a mixture of hydrogen fluoride (HF) and deionized water (1:5) at room temperature during 30 min, and rinsed in deionized water. At the beginning of the growth procedure, the Si(111) substrates were thermally etched to remove the natural SiO₂ and unintentionally formed SiN_x layer at 1120 °C in a H₂ ambient during 10 min. During the growth, trimethylgallium (TMGa), trimethylaluminum (TMAI), and ammonia (NH₃) were used as alkyl precursors for Ga, Al, and N, respectively. A nucleation AlN layer (~100 nm), an interlayer Al_xGa_{1-x}N (~10 nm), and a superlattice Al_yGa_{1-y}N/GaN ($x > y$) (~80 nm) were successively deposited in order to prevent the severe tensile stress and consequent cracking that would result from the thermal expansion coefficient difference between GaN and Si. Finally, the u-GaN epilayer of ~1.2 μm thickness was grown at 1040 °C. A schematic of the sample structure is given in Fig. 1.

^{a)}Electronic mail: Mireille.Cuniot-Ponsard@institutoptique.fr

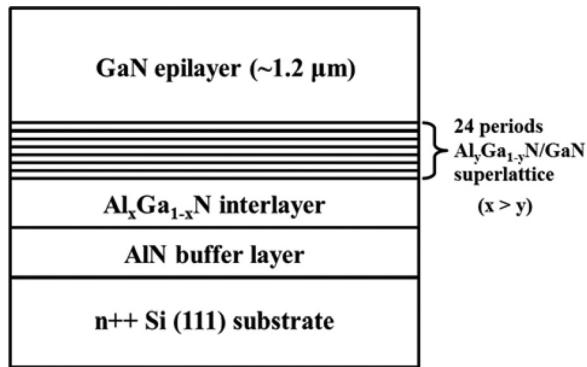


FIG. 1. Schematic diagram of the sample structure of GaN epilayer on Si(111) substrate.

Structural properties of the GaN/Si sample have been studied by high-resolution X-ray diffraction (HRXRD, X'Pert-PRO MRD), scanning electron microscopy (SEM, JEOL ULTRA 55), transmission electron microscopy (TEM, FEI Tecnai G220), and atomic force microscope (AFM, Nano-Probe instrument). Figure 2(a) shows the XRD rocking curve (ω -scan) of a GaN epilayer. The full width at half maximum (FWHM) of the dominant GaN diffraction peak was measured to be as narrow as 1712 arc sec for (002) planes, while it is 3759 arc sec for (102) planes. These values are slightly larger than some recently reported.¹³ Figure 2(b) shows the cathodoluminescence (CL) spectrum at room temperature of the GaN epilayer. Contrary to the XRD ω -rocking curve that provides information on the crystalline quality across the whole depth of the film, the CL spectrum reflects the quality of the material near the surface only. An acceleration voltage of 10 kV was used to probe the optical properties of the region in GaN between the surface and 650 nm beneath the surface. The near-band-edge emission of GaN is located at 365.3 nm, which indicates a small peak red-shift (~ 1 nm) from that of strain-free GaN, due to a remaining tensile strain. Impurity-related yellow luminescence is also observed in the CL spectrum.

Although the AlGaIn/GaN superlattice and AlGaIn interlayer effectively reduce the tensile stress applied on the GaN epilayer, threading dislocations exist as can be seen in the TEM image (Fig. 3(c)). TEM analysis provides also information on the thickness of the GaN and buffer layers, which is useful for the electro-optic (EO) modeling. Measured threading dislocations density at the surface is about $4 \times 10^8 \text{ cm}^{-2}$. Most dislocations are concentrated in the AlN/AlGaIn buffer layer and near the interface between the buffer and the GaN epilayer, which confirms the crucial role of this buffer as an absorption layer for dislocations.

Optical properties of the GaN film have been investigated using the guided wave technique based on prism

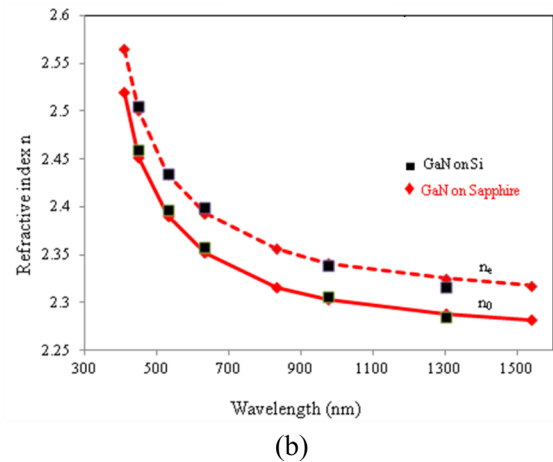
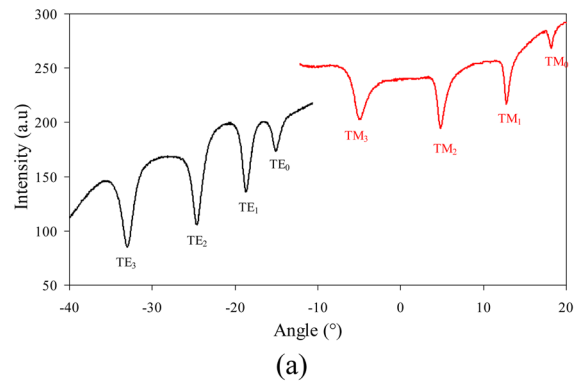


FIG. 3. Prism coupling measurements: (a) Reflectivity dips corresponding to the excitation and propagation of guided modes at $\lambda = 633$ nm in the film GaN grown on silicon. (b) Refractive index dispersion inferred from prism coupling measurements for GaN/Si and GaN/sapphire.

coupling,^{14,15} a rutile prism (TiO_2) and a Metricon M2010 setup. The reflectivity dips observed at certain angles correspond to the excitation and propagation of guided modes in the film. Figure 3(a) shows the reflectivity dips observed when the wavelength is $\lambda = 633$ nm. The sharp modes indicate a good film quality of the GaN epilayer¹⁶ and optical waveguiding is demonstrated into the GaN/Si structure. Measurements of the reflectivity in Transverse Electric (TE) and Transverse Magnetic (TM) modes were performed for different wavelengths in the range 450–1539 nm. The values of the ordinary (n_o) and extraordinary (n_e) indices of the GaN film versus wavelength are deduced and shown in Fig. 3(b). We have compared the optical properties of GaN/Sapphire and GaN/Si: the refractive indices are found quite similar. The ordinary refractive index of GaN/Si is 2.357, and its extra-ordinary refractive index is 2.392 at $\lambda = 633$ nm. The thickness of the film is deduced to be about 1248 nm, which is consistent with the TEM indication.

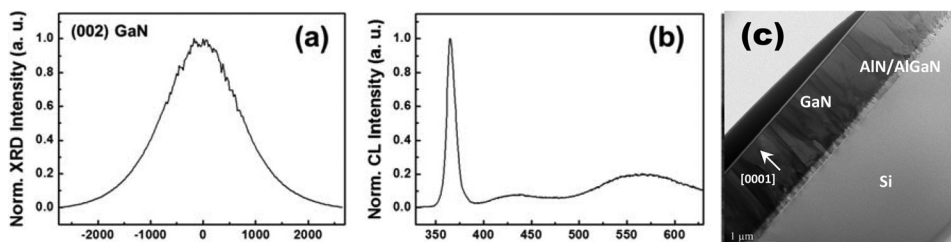


FIG. 2. (a) XRD ω -rocking curve: u-GaN on Si(111), (b) cathodoluminescence spectrum at room temperature, and (c) microstructure analysis of GaN/Si sample from TEM observation.

In order to enable the application of an electric field within the GaN film, a semi-transparent 40 nm Au top electrode was deposited by e-beam evaporation. A Ti(20 nm)/Au(200 nm) contact was deposited by sputtering directly on the n-type doped silicon substrate to form a back electrode.

The electro-optic, converse piezoelectric, and electro-absorptive coefficients of the GaN epitaxial layer have been determined simultaneously by using a method developed by Cuniot-Ponsard *et al.*¹⁷ The method exploits interferences obtained by reflection on the stack made of the GaN film sandwiched between the buffered silicon substrate and a top gold semi-transparent electrode (Fig. 4).

The reflectivity (R), and the variation in reflectivity (ΔR) induced by an alternating voltage applied between top and bottom electrodes, are measured versus incident angle (θ) successively for the TE and TM polarizations of the light. The electric-field-induced response ΔR results from the electro-optic, converse piezoelectric, and electro-absorptive effects and may be expressed as

$$\Delta R_{TE,\theta} = \left(\frac{\partial R}{\partial n_o} \right)_{TE,\theta} \Delta n_o + \left(\frac{\partial R}{\partial e} \right)_{TE,\theta} \Delta e + \left(\frac{\partial R}{\partial k_o} \right)_{TE,\theta} \Delta k_o, \quad (1)$$

$$\Delta R_{TM,\theta} = \left(\frac{\partial R}{\partial n_\theta} \right)_{TM,\theta} \Delta n_\theta + \left(\frac{\partial R}{\partial e} \right)_{TM,\theta} \Delta e + \left(\frac{\partial R}{\partial k_\theta} \right)_{TM,\theta} \Delta k_\theta, \quad (2)$$

where Δe , Δn_o , Δk_o , Δn_θ , and Δk_θ are the electric-field-induced variations of, respectively, the GaN film thickness e , its ordinary refractive index n_o and extinction coefficient k_o , its θ dependent refractive index n_θ , and extinction coefficient k_θ for TM polarization. The calculation of the reflectivity R and its derivatives is performed from Fresnel formulae by taking into account all of the multi-reflection effects in the stack. The values of the parameters (thickness and complex index) of each layer in the stack are refined thanks to the measurement of $R(\theta)$. The determination of the three unknowns Δn_o , Δe , Δk_o appearing in (1) is then achieved by selecting three experimental data [$\Delta R_{TE}(\theta_1)$, $\Delta R_{TE}(\theta_2)$, $\Delta R_{TE}(\theta_3)$] and solving the inferred system of three linear equations. The solution is necessarily unique. The unknown

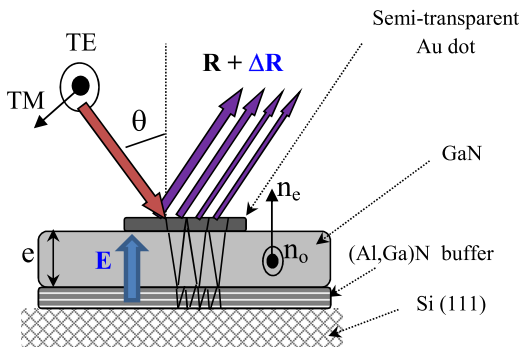


FIG. 4. Principle of the electro-optic measurement. Reflectivity (R), and variation in reflectivity (ΔR) induced by a modulating voltage (E), are measured versus incident angle θ , successively for transverse electric TE and transverse magnetic TM light polarizations

Δn_θ is then determined from the measurement of ΔR_{TM} at an angle where the derivative $\left[\frac{\partial R}{\partial k_\theta} \right]_{TM} = 0$.

The dependence of the ΔR_{TE} and ΔR_{TM} responses on the applied electric field amplitude (ΔE) is measured perfectly linear in the range 0–8.3 kV/cm. The effects involved in the field-induced response are therefore necessarily linear effects. The electro-optic Pockels coefficients r_{13} and r_{33} , as well as the converse piezoelectric coefficient d_{33} of the GaN layer can be deduced using the following expressions:

$$r_{13} = \frac{-2}{n_o^3} \frac{\Delta n_o}{\Delta E}, \quad r_{33} = \frac{-2}{n_\theta^3 \sin^2 \theta_r} \frac{\Delta n_\theta}{\Delta E} - r_{13} \cot^2 \theta_r, \quad (3)$$

$$d_{33} = \frac{\Delta e}{e \Delta E},$$

where θ_r is the refracting angle of the light wave in GaN.

The phase of the synchronously detected signal ΔR indicates that Δe is positive when the applied electric field direction is the outward normal to the substrate. This is consistent only with one of the two possible polarities for the GaN layer:¹⁸ the GaN layer is necessarily a [0001] Ga-face material with a polarization vector along the c-axis of the wurtzite structure directed towards the substrate. The sign of the electro-optic and converse piezoelectric coefficients can therefore be determined unambiguously. The values found for these coefficients when using a modulation frequency of 230 Hz are $r_{13} = +1.00 \pm 0.02$ pm/V, $r_{33} = +1.60 \pm 0.05$ pm/V at 633 nm, and $d_{33} = +4.59 \pm 0.03$ pm/V. The value measured for the electro-absorptive variation at 633 nm is $\Delta k_o/\Delta E = +0.77 \pm 0.05$ pm/V.

These results can be easily checked true by reversely calculating the electro-optic, converse piezoelectric, and electro-absorptive contributions and their sum $\Delta R(\theta)$ in the whole θ range using the above values for the coefficients. The calculated and experimental $\Delta R(\theta)$ must coincide in the whole θ range for the TE and TM polarizations of the light, and not only at the three angles used for the determination of the coefficients. Figure 5 shows the three contributions and their sum $\Delta R(\theta)$ calculated for TE polarization from the coefficients values determined in this work. Figure 6

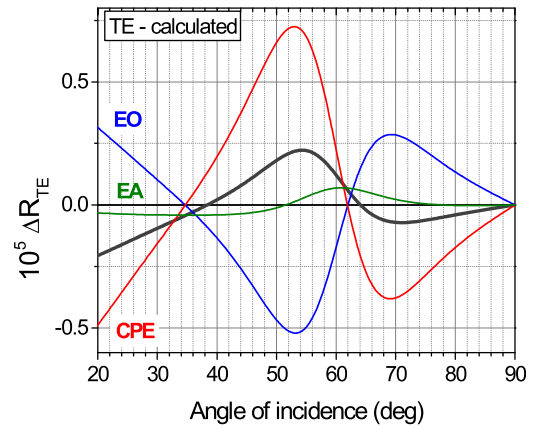


FIG. 5. Electro-optic (EO), converse-piezoelectric (CPE), and electro-absorptive (EA) components of the electric-field induced variation in TE reflectivity (ΔR_{TE} , black line) calculated from the characterization procedure results. The amplitude of the applied modulated voltage is assumed to be 1 V.

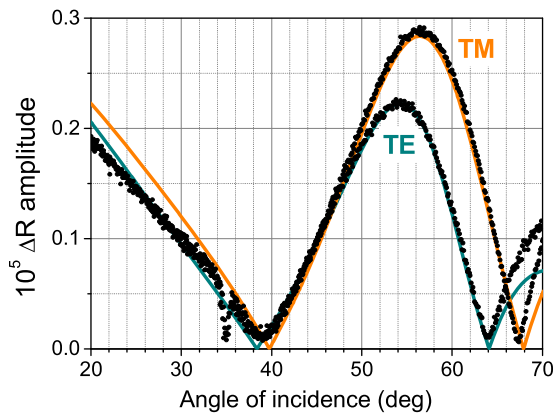


FIG. 6. Electric-field-induced variation in the reflectivity for TE and TM polarizations. Calculated (using the determined coefficients, continuous lines) and experimental data (black dots) are compared. The amplitude of the modulated voltage applied to the GaN/Si structure is 1 V.

compares the experimental and calculated $|\Delta R(\theta)|$ for both TE and TM polarizations. The agreement is very satisfying except at angles larger than 65° , where the size of the light spot on the sample exceeds that of the gold electrode so that the above model cannot account for the experimental data.

The values found here for r_{13} and r_{33} may be compared with the values $r_{13} = 0.57 \pm 0.11$ pm/V and $r_{33} = 1.91 \pm 0.35$ pm/V at 633 nm reported in the literature for GaN grown by MOCVD on sapphire and determined from Mach Zehnder measurements at 45 kHz.¹¹ Although Long *et al.*¹¹ tried to damp the electric-field induced acoustic resonances of their sample, the light phase shift induced by the converse piezoelectric effect compensated partially the phase shift induced by the electro-optic effect so that their r_{13} value is probably underestimated, and their r_{33} value consequently overestimated. The fact that Long *et al.* did not take into account the converse piezoelectric effect is the most likely explanation for the difference observed between their and our results. It must be pointed out that, due to the converse piezoelectric effect, an elasto-optic part is expected in each electro-optic coefficient: this part will collapse above the piezoelectric resonance. The converse piezoelectric coefficient ($d_{33} = +4.59 \pm 0.03$ pm/V) is found intermediate between the two values of bulk GaN ($d_{33} = +3.7$ pm/V) and bulk AlN ($d_{33} = +5.6$ pm/V).¹⁹ Interferometric measurements of this coefficient can be found in the literature for polycrystalline GaN/Si ($d_{33} = +2.0 \pm 0.1$ pm/V),²⁰ epitaxial GaN/SiC ($d_{33} = +2.8 \pm 0.1$ pm/V),¹⁹ and epitaxial GaN/AlN/Si ($d_{33} = +2.65 \pm 0.1$ pm/V).²¹ In these interferometric

measurements, the electro-optic effect is neglected, although it compensates partially the converse piezoelectric effect. The previously reported coefficient d_{33} is for this reason probably underestimated. A Piezoresponse Force Microscopy (PFM) measurement has also been reported for epitaxial GaN/AlN/SiC ($d_{33} = 2.0 \pm 1$ pm/V).²² It is to be noted that this coefficient d_{33} of III-nitrides is about one order of magnitude higher than in other III-V compounds. In conclusion, compared to other semiconductors, GaN deposited on buffered silicon appears as particularly promising for electro-optic and piezoelectric applications.

¹S. Nakamura and G. Fasol, *The Blue Laser Diode: GaN Based Light Emitters and Lasers* (Springer, Berlin, 1997).

²F. Medjdoub, B. Grimbert, D. Ducatteau, and N. Rolland, *Appl. Phys. Express* **6**, 044001 (2013).

³A. Ohtani, K. S. Stevens, and R. Beresford, *Appl. Phys. Lett.* **65**(1), 61 (1994).

⁴F. Bernardini, V. Fiorentini, and D. Vanderbilt, *Phys. Rev. B* **56**(16), R10024 (1997).

⁵J. Miragliotta, D. K. Wickenden, T. J. Kistenmacher, and W. A. Bryden, *J. Opt. Soc. Am. B* **10**, 1447 (1993).

⁶H. Y. Zhang, X. H. He, Y. H. Shih, M. Schuman, Z. C. Feng, and R. A. Stall, *Appl. Phys. Lett.* **69**, 2953 (1996).

⁷W. E. Angerer, N. Yang, A. G. Yodh, M. A. Khan, and C. J. Sun, *Phys. Rev. B* **59**, 2932 (1999).

⁸T. Fujita, T. Hasegawa, M. Haraguchi, T. Okamoto, M. Fukui, and S. Nakamura, *Jpn. J. Appl. Phys., Part 1* **39**, 2610 (2000).

⁹D. Passeri, M. C. Larciprete, A. Belardini, S. Paolini, A. Passaseo, C. Sibilia, and F. Michelotti, *Appl. Phys. B* **79**, 611 (2004).

¹⁰N. A. Sanford, A. V. Davydov, D. V. Tsvetkov, A. V. Dmitriev, S. Keller, U. K. Mishra, S. P. DenBaars, S. S. Park, J. Y. Han, and R. J. Molnar, *J. Appl. Phys.* **97**, 053512 (2005).

¹¹X. C. Long, R. A. Myers, S. R. J. Brueck, R. Ramer, K. Zheng, and S. D. Hersee, *Appl. Phys. Lett.* **67**, 1349 (1995).

¹²S. Shokhovets, R. Goldhahn, and G. Gobsch, *Mater. Sci. Eng. B* **93**, 215 (2002).

¹³J. Lin, S. Huang, Y. Su, and C. Hsu, *J. Cryst. Growth* **370**, 273 (2013).

¹⁴R. Ulrich and R. Torge, *Appl. Opt.* **12**, 2901 (1973).

¹⁵A. Stolz, E. Cho, E. Dogheche, Y. Androussi, D. Troade, D. Pavlidis, and D. Decoster, *Appl. Phys. Lett.* **98**(16), 161903 (2011).

¹⁶S. Pezzagna, J. Brault, M. Leroux, J. Massies, and M. de Micheli, *J. Appl. Phys.* **103**, 123112 (2008).

¹⁷M. Cuniot-Ponsard, J. M. Desvignes, A. Bellemain, and F. Bridou, *J. Appl. Phys.* **109**, 014107 (2011).

¹⁸O. Ambacher, J. Smart, J. R. Shealy, N. G. Weimann, K. Chu, M. Murphy, W. J. Schaff, L. F. Eastman, R. Dimitrov, L. Wittmer, M. Stutzmann, W. Rieger, and J. Hilsenbeck, *J. Appl. Phys.* **85**(6), 3222 (1999).

¹⁹I. L. Guy, S. Muensit, and E. M. Goldys, *Appl. Phys. Lett.* **75**(26), 4133 (1999).

²⁰S. Muensit and I. L. Guy, *Appl. Phys. Lett.* **72**(15), 1896 (1998).

²¹C. M. Lueng, H. L. W. Chan, C. Surya, and C. L. Choy, *J. Appl. Phys.* **88**, 5360 (2000).

²²B. J. Rodriguez, A. Gruverman, A. I. Kingon, and R. J. Nemanich, *J. Cryst. Growth* **246**, 252 (2002).